

*Letter to the Editor***Truncated disks – advective tori solutions around BHs****I. The effects of conduction and enhanced Coulomb coupling****A. Hujeirat and M. Camenzind**

Landessternwarte Königstuhl, Königstuhl 12, 69117 Heidelberg, Germany

Received 28 September 2000 / Accepted 10 October 2000

Abstract. We present the first 2D quasi-stationary radiative hydrodynamical calculations of accretion flows onto BHs taking into account cooling via Bremsstrahlung, Compton, Synchrotron and conduction. The effect of enhanced Coulomb coupling is investigated also.

Based on the numerical results obtained, we find that two-temperature (2T) accretion flows are best suited to describe hard states, and one-temperature (1T) in the soft states, with transition possibly depending on the accretion rate. In the 2T case, the ion-conduction enlarges the disk-truncation-radius from 5 to 9 Schwarzschild radii (R_S). The ion-pressure powers outflows, hence substantially decreasing the accretion rate with decreasing radius. The spectrum is partially modified BB with hard photons emitted from the inner region and showing a cutoff at 100 keV.

In the 1T case, conduction decreases the truncation radius from 7 to 5 R_S and lowers the maximum gas temperature. The outflows are weaker, the spectrum is pre-dominantly modified BB and the emitted photons from the inner region are much harder (up to 175 keV). In both cases, the unsaturated Comptonization region coincides with the transition region between the disk and the advective torus.

When gradually enhancing the Coulomb coupling, we find that the ion-temperature T_i decreases and the electron temperature T_e increases, asymptotically converging to 1T flows. However, once the dissipated energy goes into heating the ions, ion-electron thermal decoupling is inevitable within the last stable orbit (R_{MS}) even when the Coulomb interaction is enhanced by an additional two orders of magnitude.

Key words: magnetic fields – Magnetohydrodynamics (MHD) – accretion, accretion disks – black hole physics – hydrodynamics – methods: numerical

1. Introduction

Recent X-ray observations reveal that optically thick disks in AGN and LMXBs truncate within (10-100) R_S (Gilfanov et al.

1999, see also Frontera et al. 2000 and the references therein). The theoretical studies on the other hand predict a truncation radius R_{tr} between $(10^2 - 10^4)R_S$ (Narayan & Yi 1995, see also Abramowicz et al. 1998 and the references therein). Although conduction plays a key role in the disk-corona interaction, and specifically in evaporating the innermost part of the disk, and hence determining the transition radius, it has been considered only within the context of 1D or 1+1D (Meyer et al. 2000; Różańska & Czerny 2000). The transition radii in the latter studies did not differ significantly from those in the formers.

Very recently, Hujeirat & Camenzind (2000a, b, henceforth HCa, b) presented new numerical solutions based on solving the 2D problem self-consistently. They showed that, in the absence of conduction, the disk truncates close to the last stable orbit, to form a hot sub-keplerian and advective ion torus. The disk here is multi-layered and outflows are powered by ion-pressure and centrifugal barriers.

Another problem related to the validity of the 2T description of magnetized accretion flows is whether other mechanisms that are faster than Coulomb interaction may exist, forcing the ions and electrons to be in thermal equilibrium. Collective plasma waves (Begelman & Chiueh 1988) and magnetic reconnection (Bisnovaty-Kogan & Lovelace 2000) were suggested, but their applicabilities to disk-torus accretion around BHs are still not verified. On the other hand, Esin et al. (1996) found that their 1T self-similar one-dimensional solutions are not only inconsistent with the low-luminosities observed in LMXBs and AGN, they even produce “unusual” disk structure.

In this letter, the effects of the ion- and electron-conduction, as well as the sensitivity of the obtained configuration to coupling enhancement are investigated. These results are obtained using the 2D robust implicit radiative hydrodynamical solver IRMHD2 in spherical coordinates (Hujeirat 1998).

2. Governing equations, initial and boundary conditions

The set of equations and boundary conditions used here are identical to those in HCb. Further, we use the previous solutions they obtained to initiate the present runs. Using axi-symmetry, HCb solve the radiative hydrodynamical equations consisting

Send offprint requests to: A. Hujeirat

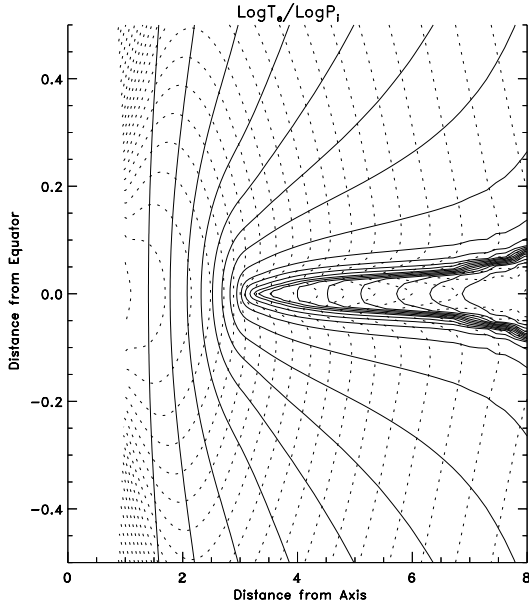


Fig. 1. Conductive-2T model. 35 uniformly, logarithmically scaled isotherms of the electron temperature (solid lines) and of the ion-pressure (dotted lines). Distances are given in units of $2.75 R_S$.

These solutions are obtained after 5000 orbital periods (in units of the orbital period at $2.75 R_S$ around a $10 M_\odot$ black hole). A material flux of $\dot{M} = 10^{17} \text{ g s}^{-1}$ is set to enter the domain of integration through the outer boundary. In this model, cooling via relativistic Bremsstrahlung, Compton and synchrotron emission, ion- and electron conduction are incorporated.

Apparently, the disk is geometrically thin, optically thick (to scattering) and surrounded by hot electrons from beneath and from above. It truncates at $R_{\text{tr}} \approx 9 R_S$ to form an optically thin non-spherical ion-torus in the inner region.

of the continuity equation for the density, Euler’s equations for three momenta, two equations for the internal energies of the ions and electrons, and one equation for the energy density of the radiation field.

In the radiation density equation, HCb modified the opacity κ such that the radiation-matter collisional term $\Lambda_B \doteq \kappa \rho (T^4 - E)$ reduces to pure relativistic Bremsstrahlung $A \rho^2 T^{1/2} + B \rho^2 T$ in optically thin regions (Stepney & Guilbert 1983) and to the radiative diffusion operator for higher optical depths. Here ρ , T and E denote the density, temperature, density of radiation and A and B are constant coefficients. Synchrotron cooling (Λ_S) and Compton cooling (Λ_C) are incorporated as well.

Here, we further include in the ion- and electron-energy equations the corresponding second order conductive operators: $L_{\{i,e\}}^2 = \nabla \cdot \kappa_{i,e} \nabla T_{i,e}$, where $\kappa_i = 3.2 \times 10^{-8} T_i^{5/2}$ and $\kappa_e = 7.8 \times 10^{-7} T_e^{5/2}$ in cgs units. The subscripts i and e denote ions and electrons respectively (see Sandbæk & Leer 1994).

Gravity of the central object is described in terms of the quasi-newtonian potential of Paczynski & Wiita (1980). A central $10 M_\odot$ black hole is assumed and an accretion rate of $-\dot{M} = 10^{17} \text{ g s}^{-1}$ is set to enter the domain $D = [0 \leq \theta \leq$

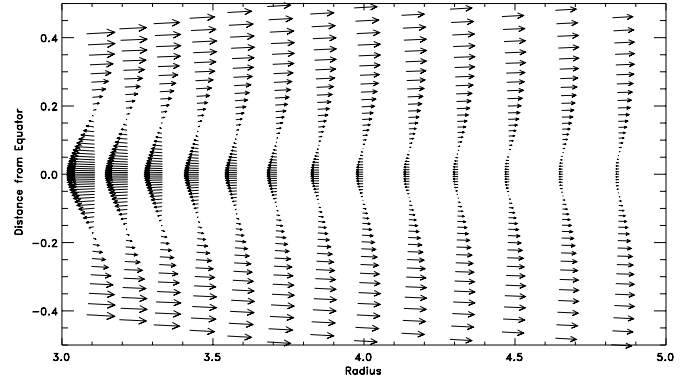


Fig. 2. Conductive-2T model. The velocity field across the transition region. The inwards motions close to the equator and the outwards oriented motion in the transition between the corona and the disk are shown also.

$\pi/2] \times [1 \leq r \leq 10]$ via a thin disk across the outer boundary. The radii in the following are measured in units of $2.75 R_S$.

In the 2T description (Shapiro et al. 1976), turbulent dissipation heats up the ions only, and subsequently the electrons via Coulomb interaction. For the dynamical viscosity we use $\eta_t = \rho \nu_t = \rho \alpha V_S H$ as the turbulent diffusion coefficient, where $H = 0.1r$ and $\alpha = 0.1$ are used.

The calculations are run till the maximum time-independent residual Res_2 has dropped below a certain small value ϵ_c . This corresponds to several thousand orbital periods of the inner radius.

3. The effects of conduction and enhanced Coulomb coupling

In a previous paper (HCb) we have shown that, in the absence of conduction, the disk truncates close to the last stable orbit for a variety of accretion rates, forming a hot ion torus around the central BH. When conduction is included, three different flow regions have been identified. There is an outer region, characterized by a Keplerian velocity, $T_i (= T_e)$ which increases inwards slightly, where radiation is the dominant cooling process, the Compton-Y parameter is large, conduction is negligible and the cooling time equals the heating time (Fig. 3, 4 and 5). There is a torus region, characterized by a hot ion plasma which rotates at sub-keplerian velocities, is optically thin, has a small Compton-Y, $T_i \gg T_e$ and the heating time decreases inwards becoming considerably smaller than the cooling time close to the inner radius. The ions here cool via advection and conduction (Fig. 3, 4 and 5).

The third region is within R_{MS} . The flow here is super-thin, isothermal and the gradient of the rotational velocity decreases strongly inwards, thereby slowing the heating- relative to the cooling-rate (Fig. 4). Both fluids cool via advection and conduction, but the electrons continue to cool efficiently via Comptonization also.

The ratio of ion- to electron-conduction time scale is $\tau_i / \tau_e \approx (\kappa_e / \kappa_i) \times (T_e / T_i)^{5/2}$. Thus, for $T_i \geq 3 \times T_e$, which can be easily maintained in 2T flows, the ion-conduction largely ex-

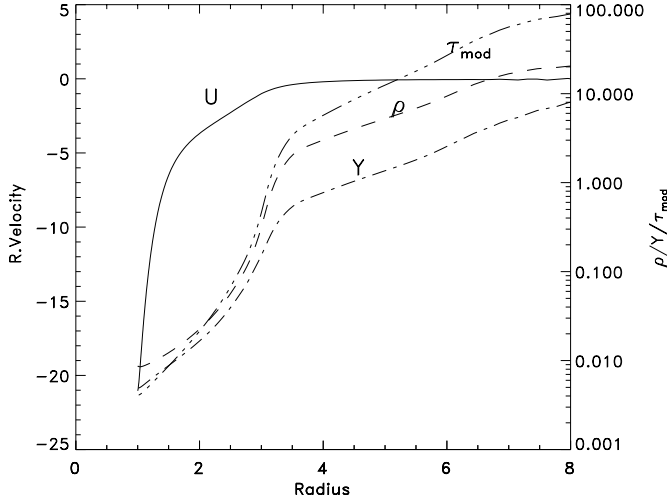


Fig. 3. The profiles of the radial velocity U (in units of $8.3 \times 10^7 \text{ cm s}^{-1}$ /left axis), density ρ in $1.45 \times 10^{-6} \text{ gr cm}^{-3}$, modified optical depth $\tau_{\text{mod}} (\doteq \int \rho(\sigma + \kappa_{\text{ff}}) ds)$ and the Compton Y -parameter ($= (4kT/mc^2) \text{Max}(\tau_{\text{es}}, \tau_{\text{es}}^2)$), right axis) along the equator. Note the rapid acceleration and the strong decrease of the variables in the torus region.

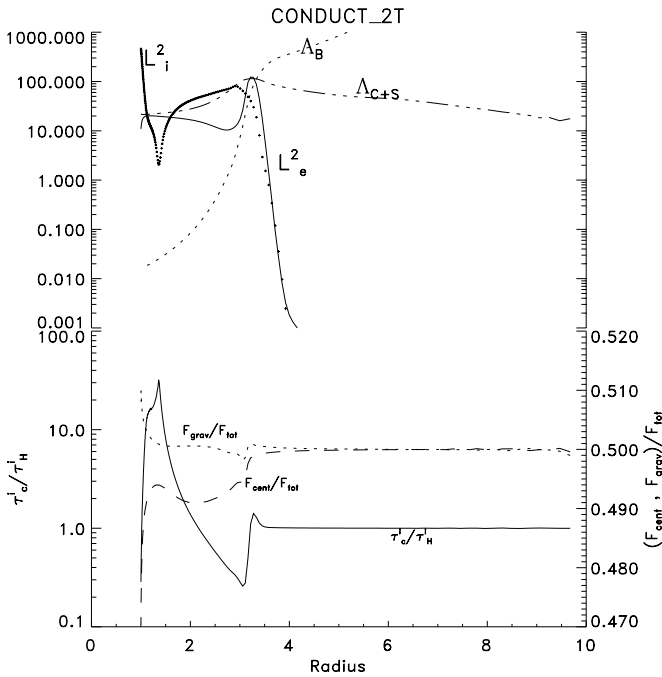


Fig. 4. Radial profiles of the ion- and electron-conduction $L_{i,e}^2$, radiative Λ_B , Compton and the synchrotron cooling Λ_{C+S} (top). The bottom figure shows the centrifugal force F_{cent} (right axis/dashed line) and gravitational force F_{grav} (dotted line) normalized to $F_{\text{tot}} (\doteq \text{gravitational} + \text{centrifugal} + \text{gas} + \text{radiative forces})$. Note that $F_{\text{grav}} \approx F_{\text{cent}} \approx 1/2 \times F_{\text{tot}}$ almost everywhere save the torus region where the ions rotate sub-keplerian. The solid line in the bottom figure shows the radial distribution of the ratio of the ion cooling time to the heating time. Note the relatively long cooling time of the ions in the torus region justifying the use of 2T description.

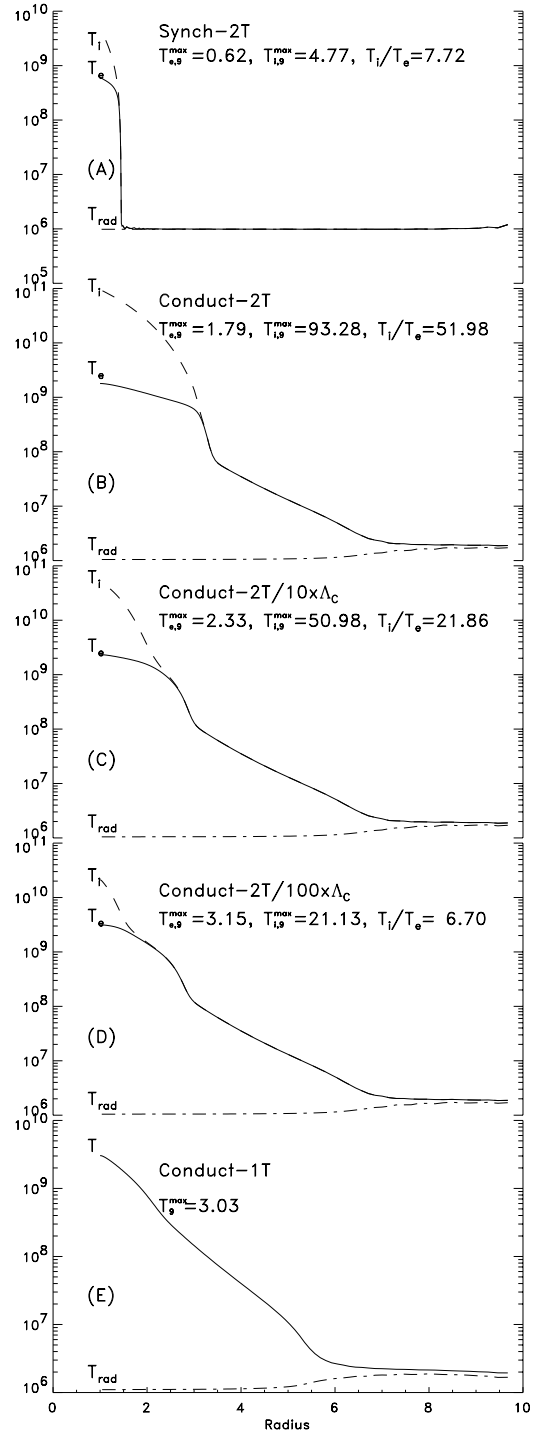


Fig. 5. The quasi-stationary profiles of the ion, electron and radiative temperatures along the equator for different models. In panel A (top) we show the initial distribution of T_i , T_e and T_{rad} obtained without conduction and which are used to initiate the subsequent models. The maximum of T_e , T_i in units of 10^9 K and their corresponding ratios are assigned as well. Panel B corresponds to the model with conduction. In C, the three profiles are shown when the Coulomb coupling is enhanced by one order of magnitude. In D the Coulomb coupling is enhanced by two orders of magnitude, and E corresponds to the 1T accretion flows. Note the increase of T_e , decrease of T_i and their convergence to 1T flows with the Coulomb enhancement.

ceeds that of the electrons. In the torus region the radial velocity $U(r) \propto R_{\text{tr}}^{-1/2}$, and since conduction increases R_{tr} , it follows that $\rho(r) \propto R_{\text{tr}}^{-3/2}$, hence the Coulomb interaction term $\Lambda_{i-e} \propto R_{\text{tr}}^{-3}$. This implies that the weakest coupling starts from the innermost region and propagates outwards.

Consequently, a considerable heat flux is carried out from this region via conduction which goes to heat the ions in the innermost part of the disk, and subsequently increasing T_e via Coulomb interaction. Since ν_{tur} increases with increasing T_i , the matter starts to accelerate, decreasing thereby the density, and subsequently weakening the radiative cooling and the Coulomb coupling ($\Lambda_{i-e} \propto \rho^2/T_e^{1/2}$) (Fig. 4). Therefore, the ion-torus expands and the truncation radius moves outwards and settles at approximately $9 R_S$.

Across R_{tr} , the Compton-Y parameter is close to unity, ion- and electron-conduction and the modified Compton cooling are efficient. Soft photons are compton-upscattered by hot electrons with temperatures ranging between $(3 - 15) \times 10^8 \text{K}$.

In the 1T case, conduction, as expected, lowers the maximum temperature in the hot torus and heats up the incoming matter from the disk. Therefore, the effect of advection becomes significant inducing an inwards shift of the truncation radius from 7 to 5 R_S . In this case unsaturated Comptonization region penetrates deeper. The soft photons here are copious and efficiently compton-upscattered by more energetic electrons than in the 2T case (T_e in this region ranges between $(1 - 3) \times 10^9 \text{K}$).

Furthermore, the pressure gradient is two orders of magnitude smaller and therefore gives rise to less powerful outflows than in the 2T case. Across the inner boundary, the gas speed is subsonic relative to T_i whereas it is supersonic in the 1T case. This may explain why the accretion rate decreases inwards much more strongly in the 2T than in the 1T case.

We note that our 1T results disagree principally with the ‘unusual’ flow structure obtained by Esin et al. (1996). Here, the 1T is as good as the 2T description in forming a truncated disk-advective torus and providing a temperature range that can be well accommodated within the observational data of Cyg X-1 in its high state. Fig. 5 shows that the stronger the ion-electron coupling, the lower is T_i , the higher T_e , and the closer they become to the 1T accretion flows. However, we have assumed that the electron and ion mean molecular weight remain unchanged as the coupling strength is enhanced.

We note that in both cases the temperature-increase in the inner region is much stronger than in the disk (more than $r^{-3/4}$).

This implies that conduction can easily supply the required energy to maintain a smooth transition from an optically thick disk to an optically thin advective torus (Fig. 5).

The observational relevance of our results are twofold. We suggest that 1T descriptions are more appropriate for accretion flows at higher rates. We expect outflows and winds to be less powerful, a pronounced modified BB spectrum and that the hard photons are well represented by a power law profile with a cutoff at 150 – 200 keV. On the other hand, powerful outflows and winds, R_{tr} between $(8 - 10) R_S$, a less pronounced modified BB spectrum and a power law spectrum describing the hard photons with a cutoff at 80 – 100 keV are signatures for 2T accretion flows. This implies that the overall bolometric luminosity here is considerably lower than in the former case.

When the accretion rate is enhanced due to external mechanisms, the density increases, thereby enhancing the ion-electron thermal coupling, and allowing a transition from a 2T to 1T flow. In this case, the torus shrinks in volume only (but it continues to survive within R_{MS}), and the disk moves inwards, truncating between $(3 - 5) R_S$.

Acknowledgements. AH’s research has been supported by the Deutsche Forschungsgemeinschaft (DFG) through the Schwerpunktprogramm *Physik der Sternentstehung*. Computations were performed on IWR-facilities at the University of Heidelberg and the Landessternwarte-Königstuhl in Heidelberg.

References

- Abramowicz, M., Igumenshchev, I.V., Lasota, J-P., 1998, MNRAS, 293, 443
- Begelman, M.C., Chiueh, T., 1988, ApJ, 332, 873
- Bisnovatyi-Kogan, G.S., Lovelace, R.V.E., 2000, ApJ, 529, 978
- Esin, A. A., Narayan, R., et al., 1996, ApJ, 465, 312
- Frontera, F, Palazzi, E, et al. 2000, Astro-ph/0009160
- Gilfanov, M., Churazov, E., Revnivtsev, M., 2000, Astro-ph/0001450
- Hujeirat, A., 1998, MNRAS, 298, 320
- Hujeirat, A., Camenzind, M., 2000a, A&A Letters, 360, L17
- Hujeirat, A., Camenzind, M., 2000b, A&A Letters, in press
- Meyer, F., Liu, B.F., Meyer-Hofmeister, E., 2000, Astro-ph/0002053
- Narayan, R., Yi, I., 1995, ApJ, 444, 231
- Paczynski, B., Wiita, P.J., 1980, A&A, 88, 23
- Różańska, A., Czerny, B., 2000, Astro-ph/0004158
- Sandbæk, Ø., Leer, E., 1994, ApJ, 423, 500
- Shapiro, S.L., Lightman A.P., Eardley, D.M., 1976, ApJ, 204, 187
- Stepney, S., Guilbert, P.W., 1983, MNRAS, 204, 1269